

# Improving the protection system in the distribution networks integrated with photovoltaic cells by changing the ratio of X/R

Muhanad N. Ali<sup>1</sup>, Othman M. K. Alsmadi<sup>2,3</sup>, Ali M. Baniyounes<sup>4</sup>

<sup>1</sup>Solar Power Plant, Anbar, Iraq

<sup>2</sup>Department of Electrical Engineering, Faculty of Engineering, Al-Ahliyya Amman University, Amman, Jordan

<sup>3</sup>Department of Electrical Engineering, School of Engineering, The University of Jordan, Amman, Jordan

<sup>4</sup>Electrical Engineering Department, Faculty of Engineering and Technology, Applied Science Private University, Amman, Jordan

## Article Info

### Article history:

Received Apr 21, 2022

Revised Oct 23, 2023

Accepted Nov 7, 2023

### Keywords:

Distance relay

Distribution generation

ETAP

Overcurrent relay

Photovoltaic energy

Power system

Protection system

## ABSTRACT

Due to the increased demand for electrical energy, many countries were prompted nowadays to search for new sources. One important source is the photovoltaic energy. However, despite the great benefits of this source, some defects were observed when linking to distribution networks (negative impact on the protection system). Hence, an approach of improving the protection system in distribution networks integrated with photovoltaic cells is presented in this paper. The protection system improvement is proposed by changing the impedance to resistance ratio (X/R) values of the networks cables, which leads to increasing the overcurrent relays' response speed when a fault occurs. A comparative analysis with different cable reactance values was conducted. The electrical transient analyzer program (ETAP) software was used to investigate and validate the effects on the relay's response times. Amriya Fallujah power station, located in Iraq, was investigated as a case study. Simulation results show that it is possible to increase the response speed of the overcurrent relay by reducing X/R of the network cables. For more validation, the distance relay was used to compare the best improvement results of changing the X/R ratio with the results of changing the type of relay, which also shows the strength of the proposed method.

*This is an open access article under the [CC BY-SA](https://creativecommons.org/licenses/by-sa/4.0/) license.*



## Corresponding Author:

Othman M. K. Alsmadi

Department of Electrical Engineering, Faculty of Engineering, Al-Ahliyya Amman University

Amman, 19328 Jordan

Email: othmanmk@ju.edu.jo

## NOMENCLATURE

PV : Photovoltaic

MG : Micro-grid

ETAP : Electrical transient analyzer program

DG : Distributed generation

GHG : Greenhouse gas

SCADA : Supervisory control and data acquisition

IEEE : The institute of electrical and electronics engineers

ROCOF : Rate of change of frequency

SFS : Security facility services

IDMT : Inverse definite minimum time

CTI : Coordination time interval

$t$  : The operating time

TDS : Time dial setting

$t_p$  : The operating time

$I_R$  :  $I_{Input}/I_{Pickup}$

X : Reactance

R : Resistance

## 1. INTRODUCTION

In recent years, a global demand for electrical energy has increased due to the significant development in various areas [1]. This demand has led to an environmental pollution (along with other issues) caused by the increased usage of traditional energy sources, one of which as most important is the fossil fuel, which has different disadvantages. One is a negative environmental effect caused by the fossil fuel combustion which is gradually causing a climate change. Another is the high cost associated with extracting and transporting this type of fuel [2], [3]. These reasons have prompted many countries to search for new and more economical renewable energy sources that may not be linked to other specific countries to eliminate the dominance of some fossil fuel-producing countries [4], [5]. The most important sources were focused on are the photovoltaic and wind energies [6], [7]. The percentage of using such types of energy has recently increased significantly as shown in Figure 1 [8], [9].

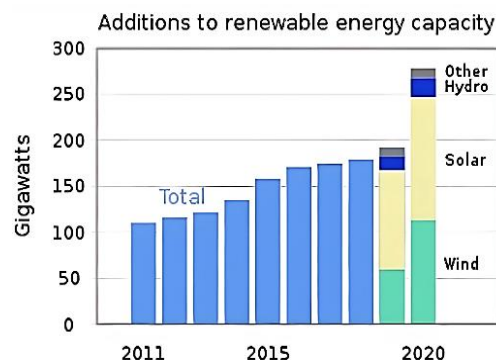


Figure 1. The increase of photovoltaic and wind energy utilization

Renewable energy systems in distribution network, especially photovoltaic (PV), creates excellent opportunities but makes the grid operation more complicated. With many factors in mind, there was a demand to provide a compelling connection between the distributed generation (DG) and the electrical network [10]. These factors include higher power factor rate, lower reactive power value, lower losses, and lower pollution as a result of higher greenhouse gas emissions (GH). In general, the electric energy exported to the electric grid has a single power factor, but the increase in the number of DGs and their penetration into the electric grid can cause some problems [11].

One of these problems is its impact on the protection system and the change in the energy flow. Several methodologies have been widely used to maintain higher protection standards for the electrical grid-connected DG system. These approaches include multilevel inverters, static variance compensators, power control strategies (such as electric vehicle charging systems), artificial intelligence, power switching electronics, and supervisory control systems and data acquisition (SCADA), which is used for distribution, transmission, and power relays [12], [13].

In this paper, the impact of changing X/R ratio of the network cables on the network stability and on enhancing the response speed of the overcurrent relay is discussed. The variation of the X/R ratio, whether increasing or decreasing, exerts a notable effect on the overcurrent relay's response speed. This impact is validated by the simulation results obtained by electrical transient analyzer program (ETAP). Cable reactance values were deliberately modified, with selection and analysis based on values provided by manufacturers, for the purpose of identifying the optimal value that accelerates the relay response to faults [14], [15]. Furthermore, to explore the efficacy of using distance relays as an alternative to overcurrent relays, investigating the potential and extent of their impact on expediting the response to faults in distribution networks.

## 2. EFFECT OF X/R RATIO IN DISTRIBUTION NETWORKS

As mentioned earlier, altering the X/R ratio can significantly impacts the response speed of the relays, and hence influencing the network stability, particularly in distribution networks [16], [17]. The X/R ratio is influenced by the impedance of the transformers and lines within these networks. Since the lines design and the choice of conductor type hinge primarily on two factors, which are the current and voltage drop, it is important to note that these factors differ between transmission and distribution lines. In

transmission lines, current takes precedence due to its greater magnitude, whereas in distribution networks, voltage drop is more significant owing to the comparatively lower current. Kim *et al.* [18], presented that the lower the current density, the higher the inductor cross-sectional area, which leads to lower resistance values in the distribution networks. The resistance value in distribution transformers is relatively high compared to those used in transmission networks, and as a result, the total resistance value is increased in the point of common coupling (PCC). Knowing that the reactance value of the line relies on the equivalent distance (Deq) between the phases and the geometric mean radius (GMR) of the conductor [19], [20], it becomes important to highlight the direct relationship between Deq and voltage [21]. Now, given lower voltage values in distribution systems, Deq will tend to become minor, potentially decreasing the X/R ratio [22]. Hence, it is our objective in this paper to demonstrate the impact of low X/R ratio on the relay response speed while trying to achieve optimal responsiveness to network faults in the presence of integrated photovoltaic cells [23], [24].

### 3. METHODOLOGY

#### 3.1. Case study

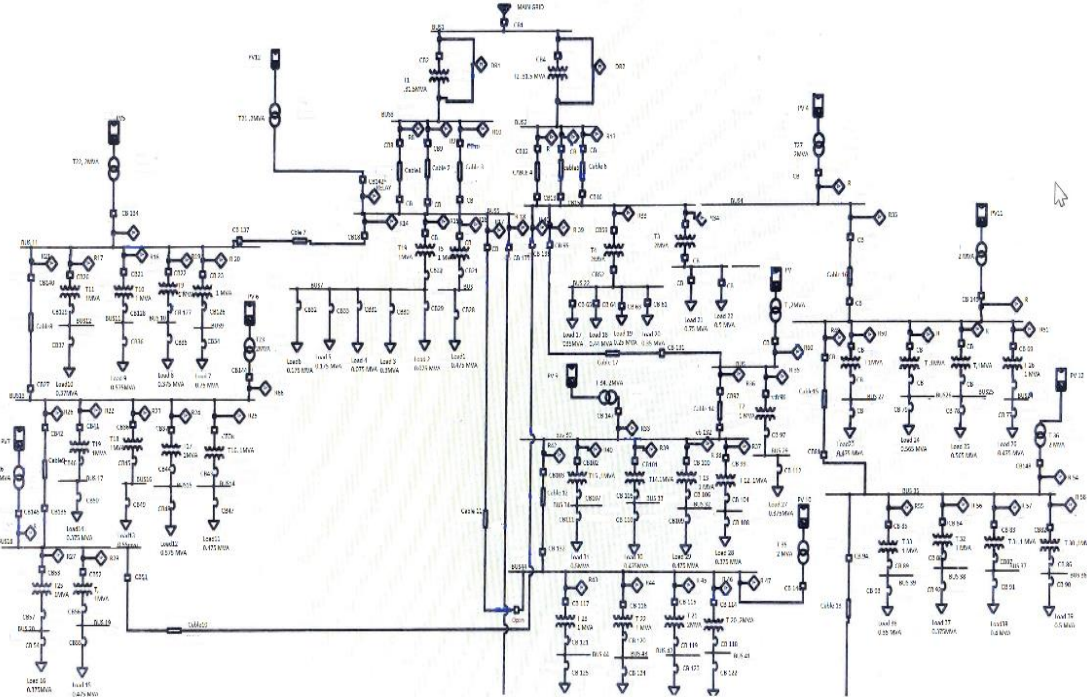
Iraq's Amriya Fallujah power station was selected as a case study to demonstrate the new approach of improving the electrical protection system. The Amriya Fallujah network comprises numerous transformers that provide electricity to residential buildings. The network is structured into secondary substations interconnected by underground cables tied to a central station. The existing protection system includes circuit breakers, overcurrent relays, and ground fault relays. The Al-Fallujah network was chosen to analyze the effects of integrating a renewable solar photovoltaic (PV) energy generation system, since connecting PV systems to electrical distribution grids can affect the protection system. Details of the various components of the Al-Fallujah electrical network are provided in Table 1.

Table 1. Major components of the electrical network.

| No. | Content             | Specifications     | Quantity |
|-----|---------------------|--------------------|----------|
| 1   | Transformer         | 31.5 MVA, 33/11 KV | 2        |
| 2   | Transformer         | 2 MVA, 11/3.4 KV   | 2        |
| 3   | Transformer         | 1 MVA, 11/0.4 KV   | 29       |
| 4   | Bus                 | 33 KV              | 1        |
| 5   | Buses               | 11 KV              | 16       |
| 6   | Buses               | 0.4 KV             | 29       |
| 7   | Buses               | 3.4 KV             | 2        |
| 8   | Loades              | 0.4 KV, 3.4 KV     | 31       |
| 9   | Over-current relays | 48                 | 44       |
| 10  | Circuit breaker     | 33 KV, 11 KV       | 33       |
| 11  | Cables              | 11 KV, 240 mm      | 149000 m |
| 12  | PV units            | 1.2 MVA            | 10       |

#### 3.2. Numerical simulation and methodology

The ETAP software package was used for numerical modeling and simulations of the overcurrent and distance relays in this case study. In the analysis process, a comparative investigation was initiated for calculating the response time of the distribution network protection relays associated with a photovoltaic (PV) system employing two distinct relay types. The initial focus was on the overcurrent relay, and then the distance relay. The study involves the introduction of three fault types in the electrical network in order to assess the response time of these relays, which were as following: i) line-to-line fault, ii) line-to-ground fault, and iii) three-phase fault. Subsequently, three different PV production ratios were applied to simulate these faults: i) operating at 50% of the total PV power, ii) operating at 75% of the total PV power, and iii) operating at 100% of the total PV power. Now, the overcurrent relay analysis comprises 27 cases, each was based on three reactance values: (i) 0.12, (ii) 0.083, and (iii) 0.185. Following the implementation of these values, coupled with the capabilities of the PV system and electrical faults, the distribution system's least-performing response time was determined by comparing the overcurrent and distance relays. Furthermore, several buses were selected to cause a range of faults to investigate the speed of responses of the overcurrent relays when X/R ratio values were changed [25], [26]. Figure 2 shows a line diagram of the Amriya Fallujah power station presented in the ETAP program.



Y: 15717 (Zoom Level: 19)

Figure 2. Single line diagram of Amriya Fallujah power station presented in ETAP program

#### 4. RESULTS AND DISCUSSION

##### 4.1. Overcurrent relay (three phase faults)

In this subsection, several three-phase faults were made in various buses in the network with a change in the ratio of X/R by choosing three values for the reactance of the cables connecting the electrical network, which were at 0.083, 0.12, and 0.185 Ohms, respectively. These faults were in three percentages of photovoltaic integration with the distribution network, where 50%, 75%, and 100% of the total power of these units were selected to determine the best response speed for the overcurrent relays, as shown in Tables 2, 3, and 4.

Table 2. 3-phase fault at bus 19

| Relay No | PV 100%         |                  |                  | PV 75%          |                  |                  | PV 50%          |                  |                  |
|----------|-----------------|------------------|------------------|-----------------|------------------|------------------|-----------------|------------------|------------------|
|          | X=0.12<br>T(ms) | X=0.185<br>T(ms) | X=0.083<br>T(ms) | X=0.12<br>T(ms) | X=0.185<br>T(ms) | X=0.083<br>T(ms) | X=0.12<br>T(ms) | X=0.185<br>T(ms) | X=0.083<br>T(ms) |
| R28      | 12.4            | 12.4             | 12.4             | 12.4            | 12.4             | 12.4             | 12.4            | 12.4             | 12.4             |
| R26      | 17.4            | 17.4             | 17.4             | 17.4            | 17.4             | 17.4             | 17.4            | 17.4             | 17.4             |
| R21      | 64.7            | 76.0             | 58.7             | 63.3            | 74.1             | 57.6             | 61.7            | 71.9             | 56.3             |
| R14      | 159             | 189              | 144              | 154             | 182              | 140              | 148             | 174              | 135              |
| R8       | 853             | 1011             | 771              | 833             | 985              | 754              | 799             | 940              | 725              |
| R9       | 853             | 1011             | 771              | 833             | 985              | 754              | 799             | 940              | 725              |
| R10      | 853             | 1011             | 771              | 833             | 985              | 754              | 799             | 940              | 725              |

Table 3. 3-phase fault at bus 14

| Relay No | PV 100%         |                  |                  | PV 75%          |                  |                  | PV 50%          |                  |                  |
|----------|-----------------|------------------|------------------|-----------------|------------------|------------------|-----------------|------------------|------------------|
|          | X=0.12<br>T(ms) | X=0.185<br>T(ms) | X=0.083<br>T(ms) | X=0.12<br>T(ms) | X=0.185<br>T(ms) | X=0.083<br>T(ms) | X=0.12<br>T(ms) | X=0.185<br>T(ms) | X=0.083<br>T(ms) |
| R25      | 12.4            | 12.4             | 12.4             | 12.4            | 12.4             | 12.4             | 12.4            | 12.4             | 12.4             |
| R21      | 57.5            | 65.0             | 53.5             | 56.5            | 63.6             | 52.6             | 55.2            | 61.9             | 51.6             |
| R14      | 141             | 160              | 130              | 137             | 155              | 127              | 132             | 149              | 123              |
| R8       | 750             | 856              | 694              | 735             | 835              | 681              | 708             | 801              | 658              |
| R9       | 750             | 856              | 694              | 735             | 835              | 681              | 708             | 801              | 658              |
| R10      | 750             | 856              | 694              | 735             | 835              | 681              | 708             | 801              | 658              |

Table 4. 3-phase fault at bus 41

| Relay No | PV 100%         |                  |                  | PV 75%          |                  |                  | PV 50%          |                  |                  |
|----------|-----------------|------------------|------------------|-----------------|------------------|------------------|-----------------|------------------|------------------|
|          | X=0.12<br>T(ms) | X=0.185<br>T(ms) | X=0.083<br>T(ms) | X=0.12<br>T(ms) | X=0.185<br>T(ms) | X=0.083<br>T(ms) | X=0.12<br>T(ms) | X=0.185<br>T(ms) | X=0.083<br>T(ms) |
| R46      | 12.4            | 12.4             | 12.4             | 12.4            | 12.4             | 12.4             | 12.4            | 12.4             | 12.4             |
| R42      | 41.0            | 42.9             | 35.9             | 40.8            | 42.5             | 35.6             | 40.5            | 42.1             | 35.4             |
| R36      | 182             | 190              | 157              | 179             | 186              | 154              | 174             | 181              | 151              |
| R32      | 389             | 408              | 332              | 378             | 395              | 324              | 364             | 379              | 313              |
| R11      | 4950            | 4950             | 4435             | 4950            | 4950             | 4485             | 4950            | 4950             | 4360             |
| R12      | 4950            | 4950             | 4435             | 4950            | 4950             | 4485             | 4950            | 4950             | 4360             |
| R13      | 4950            | 4950             | 4435             | 4950            | 4950             | 4485             | 4950            | 4950             | 4360             |

#### 4.2. Overcurrent relay (line to line faults)

Here, we will work on several (L-L) faults in multiple areas of the electrical network by changing the inductance values of the cable each time, as performed in the first case, as well as changing the rate of penetration of the photovoltaic cells of the system. This step was performed in order to see to what extent the response speeds of the relays can change and to find the best value of the inductance at which the relay response can be as fast as possible. Tables 5, 6, and 7 show the response speed of the relays.

Table 5. Line-line fault at bus 19

| Relay No | PV 100%         |                  |                  | PV 75%          |                  |                  | PV 50%          |                  |                  |
|----------|-----------------|------------------|------------------|-----------------|------------------|------------------|-----------------|------------------|------------------|
|          | X=0.12<br>T(ms) | X=0.185<br>T(ms) | X=0.083<br>T(ms) | X=0.12<br>T(ms) | X=0.185<br>T(ms) | X=0.083<br>T(ms) | X=0.12<br>T(ms) | X=0.185<br>T(ms) | X=0.083<br>T(ms) |
| R28      | 12.4            | 12.4             | 12.4             | 12.4            | 12.4             | 12.4             | 12.4            | 12.4             | 12.4             |
| R26      | 17.4            | 17.4             | 17.4             | 17.4            | 17.4             | 17.4             | 17.4            | 17.4             | 17.4             |
| R21      | 59.7            | 70.5             | 54.8             | 59.5            | 69.9             | 54.6             | 59.1            | 69.1             | 54.2             |
| R14      | 140             | 165              | 128              | 139             | 164              | 128              | 138             | 162              | 127              |
| R8       | 744             | 877              | 684              | 748             | 881              | 686              | 742             | 872              | 679              |
| R9       | 744             | 877              | 684              | 748             | 881              | 686              | 742             | 872              | 679              |
| R10      | 744             | 877              | 684              | 748             | 881              | 686              | 742             | 872              | 679              |

Table 6. Line-line fault at bus 14

| Relay No | PV 100%         |                  |                  | PV 75%          |                  |                  | PV 50%          |                  |                  |
|----------|-----------------|------------------|------------------|-----------------|------------------|------------------|-----------------|------------------|------------------|
|          | X=0.12<br>T(ms) | X=0.185<br>T(ms) | X=0.083<br>T(ms) | X=0.12<br>T(ms) | X=0.185<br>T(ms) | X=0.083<br>T(ms) | X=0.12<br>T(ms) | X=0.185<br>T(ms) | X=0.083<br>T(ms) |
| R25      | 12.4            | 12.4             | 12.4             | 12.4            | 12.4             | 12.4             | 12.4            | 12.4             | 12.4             |
| R21      | 53.5            | 59.6             | 50.3             | 53.4            | 59.4             | 50.1             | 53.1            | 59.1             | 49.8             |
| R14      | 125             | 139              | 117              | 125             | 139              | 117              | 124             | 138              | 116              |
| R8       | 661             | 734              | 621              | 665             | 741              | 624              | 661             | 738              | 619              |
| R9       | 661             | 734              | 621              | 665             | 741              | 624              | 661             | 738              | 619              |
| R10      | 661             | 734              | 621              | 665             | 741              | 624              | 661             | 738              | 619              |

Table 7. Line-line fault at bus 41

| Relay No | PV 100%         |                  |                  | PV 75%          |                  |                  | PV 50%          |                  |                  |
|----------|-----------------|------------------|------------------|-----------------|------------------|------------------|-----------------|------------------|------------------|
|          | X=0.12<br>T(ms) | X=0.185<br>T(ms) | X=0.083<br>T(ms) | X=0.12<br>T(ms) | X=0.185<br>T(ms) | X=0.083<br>T(ms) | X=0.12<br>T(ms) | X=0.185<br>T(ms) | X=0.083<br>T(ms) |
| R46      | 12.4            | 12.4             | 12.4             | 12.4            | 12.4             | 12.4             | 12.4            | 12.4             | 12.4             |
| R42      | 40.1            | 41.8             | 35.2             | 40              | 41.7             | 35.1             | 40              | 41.6             | 35.1             |
| R36      | 169             | 176              | 148              | 168             | 175              | 147              | 167             | 174              | 146              |
| R32      | 343             | 355              | 300              | 343             | 355              | 299              | 340             | 353              | 296              |
| R11      | 4555            | 4653             | 3875             | 4767            | 4908             | 4021             | 4811            | 4950             | 4040             |
| R12      | 4555            | 4653             | 3875             | 4767            | 4908             | 4021             | 4811            | 4950             | 4040             |
| R13      | 4555            | 4653             | 3875             | 4767            | 4908             | 4021             | 4811            | 4950             | 4040             |

#### 4.3. Overcurrent relay (line to ground faults)

In this subsection, we will work on several (L-G) faults in several buses in the electrical network while changing the inductance values of the cable each time, as well as changing the rate of penetration of the photovoltaic cells of the system. Similarly, this step is performed to see how quickly the response of the relays changes and to find the best value of inductance during which the response of the relay can be obtained with a minimum time. Tables 8, 9, and 10 show the response speed of the relays at each value of X in the different ratios of the photovoltaic production interference.

Table 8. Line-ground fault at bus 19

| Relay No | PV 100%         |                  |                  | PV 75%          |                  |                  | c               |                  |                  |
|----------|-----------------|------------------|------------------|-----------------|------------------|------------------|-----------------|------------------|------------------|
|          | X=0.12<br>T(ms) | X=0.185<br>T(ms) | X=0.083<br>T(ms) | X=0.12<br>T(ms) | X=0.185<br>T(ms) | X=0.083<br>T(ms) | X=0.12<br>T(ms) | X=0.185<br>T(ms) | X=0.083<br>T(ms) |
| R28      | 16.8            | 18.7             | 15.7             | 16.9            | 18.8             | 15.8             | 17              | 18.9             | 15.9             |
| R26      | 31.4            | 34.8             | 29.6             | 32.3            | 35.8             | 30.4             | 33.2            | 36.8             | 31.2             |
| R21      | 116             | 128              | 110              | 123             | 135              | 116              | 130             | 143              | 122              |
| R14      | 244             | 267              | 231              | 268             | 294              | 253              | 292             | 323              | 275              |
| R8       | 1161            | 1261             | 1105             | 1325            | 1451             | 1255             | 1500            | 1660             | 1413             |
| R9       | 1161            | 1261             | 1105             | 1325            | 1451             | 1255             | 1500            | 1660             | 1413             |
| R10      | 1161            | 1261             | 1105             | 1325            | 1451             | 1255             | 1500            | 1660             | 1413             |

Table 9. Line-ground fault at bus 14

| Relay No | PV 100%         |                  |                  | PV 75%          |                  |                  | PV 50%          |                  |                  |
|----------|-----------------|------------------|------------------|-----------------|------------------|------------------|-----------------|------------------|------------------|
|          | X=0.12<br>T(ms) | X=0.185<br>T(ms) | X=0.083<br>T(ms) | X=0.12<br>T(ms) | X=0.185<br>T(ms) | X=0.083<br>T(ms) | X=0.12<br>T(ms) | X=0.185<br>T(ms) | X=0.083<br>T(ms) |
| R25      | 22.5            | 24.4             | 21.5             | 22.6            | 24.5             | 21.6             | 22.7            | 24.6             | 21.7             |
| R21      | 108             | 116              | 104              | 114             | 123              | 109              | 120             | 130              | 115              |
| R14      | 227             | 242              | 218              | 248             | 266              | 238              | 270             | 291              | 258              |
| R8       | 1082            | 1151             | 1043             | 1228            | 1314             | 1180             | 1384            | 1491             | 1325             |
| R9       | 1082            | 1151             | 1043             | 1228            | 1314             | 1180             | 1384            | 1491             | 1325             |
| R10      | 1082            | 1151             | 1043             | 1228            | 1314             | 1180             | 1384            | 1491             | 1325             |

Table 10. Line-ground fault at bus 41

| Relay No | PV 100%         |                  |                  | PV 75%          |                  |                  | PV 50%          |                  |                  |
|----------|-----------------|------------------|------------------|-----------------|------------------|------------------|-----------------|------------------|------------------|
|          | X=0.12<br>T(ms) | X=0.185<br>T(ms) | X=0.083<br>T(ms) | X=0.12<br>T(ms) | X=0.185<br>T(ms) | X=0.083<br>T(ms) | X=0.12<br>T(ms) | X=0.185<br>T(ms) | X=0.083<br>T(ms) |
| R46      | 16.4            | 16.9             | 14.9             | 16.4            | 17               | 15               | 16.6            | 17.1             | 15.1             |
| R42      | 88.8            | 91.6             | 81.2             | 91.3            | 94               | 83.2             | 93.8            | 96.5             | 85.3             |
| R36      | 341             | 351              | 312              | 361             | 372              | 329              | 382             | 393              | 347              |
| R32      | 611             | 624              | 562              | 670             | 686              | 613              | 731             | 750              | 664              |
| R11      | 4950            | 4950             | 4950             | 4950            | 4950             | 4950             | 4950            | 4950             | 4950             |
| R12      | 4950            | 4950             | 4950             | 4950            | 4950             | 4950             | 4950            | 4950             | 4950             |
| R13      | 4950            | 4950             | 4950             | 4950            | 4950             | 4950             | 4950            | 4950             | 4950             |

#### 4.4. Distance relay

Here, a list of employed overcurrent relays and the corresponding distance relays employed in the system is summarized in Table 11. Now, the following subsections will present the response speed of the relays at each value of X in different ratios of photovoltaic production interferences. The following subsections will also present different faults being placed on different busbars.

Table 11. Different overcurrent relays with the correspondent distance relays

| Overcurrent relay | Correspondent distance relay |
|-------------------|------------------------------|
| R-14              | R-67                         |
| R-21              | R-89                         |
| R-26              | R-93                         |
| R-42              | R-103                        |
| R-36              | R-101                        |
| R-49              | R-108                        |
| R-35              | R-110                        |
| R-32              | R-99                         |

#### 4.5. Distance relay (three phase faults)

As seen next, several faults were made on several busbars, as shown in Tables 12-14. The faults are made with the presence of the distance relay on the network cables instead of the overcurrent relay. This step is performed in the event of a change in the production rate of photovoltaic cells in order to compare the results with the previous ones.

Table 12. 3-phase fault at bus 14

| Relay No | PV 100% T(ms) | PV 75% T(ms) | PV 50% T(ms) |
|----------|---------------|--------------|--------------|
| R25      | 12.4          | 12.4         | 12.4         |
| R89      | 40.6          | 39.6         | 38.8         |
| R67      | 94.6          | 94.6         | 91.6         |
| R8       | 186           | 187          | 181          |
| R9       | 1861          | 1874         | 1810         |
| R10      | 1861          | 1874         | 1810         |

Table 13. 3-phase fault at bus 19

| Relay No | PV 100% T(ms) | PV 75% T(ms) | PV 50% T(ms) |
|----------|---------------|--------------|--------------|
| R28      | 12.4          | 12.4         | 12.4         |
| R93      | 14            | 14           | 14           |
| R89      | 45.5          | 44.5         | 43.3         |
| R67      | 107           | 104          | 101          |
| R8       | 210           | 207          | 201          |
| R9       | 2134          | 2096         | 2028         |
| R10      | 2134          | 2096         | 2028         |

Table 14. 3-phase fault at bus 41

| Relay No | PV 100% T(ms) | PV 75% T(ms) | PV 50% T(ms) |
|----------|---------------|--------------|--------------|
| R46      | 12.4          | 12.4         | 12.4         |
| R103     | 31.6          | 31.4         | 31.2         |
| R101     | 140           | 137          | 134          |
| R99      | 297           | 289          | 278          |
| R11      | 4950          | 4950         | 4921         |
| R12      | 4950          | 4950         | 4921         |
| R13      | 4950          | 4950         | 4921         |

#### 4.6. Distance relay (line to line faults)

In the followings, several faults were made on several buses. Again, the distance relay was placed on the network cables instead of the overcurrent relay. This process was made in the event of changing the production rate of the photovoltaic cells in order to compare the results with the previous ones. Results are as presented in Tables 15-17.

Table 15. L-L fault at bus 14

| Relay | PV 100% T(ms) | PV 75% T(ms) | PV 50% T(ms) |
|-------|---------------|--------------|--------------|
| R25   | 12.4          | 12.4         | 12.4         |
| R89   | 38            | 37.8         | 37.5         |
| R67   | 88.3          | 88           | 87.2         |
| R8    | 173           | 174          | 172          |
| R9    | 1720          | 1726         | 1711         |
| R10   | 1720          | 1726         | 1711         |

Table 16. L-L fault at bus 19

| Relay | PV 100% T(ms) | PV 75% T(ms) | PV 50% T(ms) |
|-------|---------------|--------------|--------------|
| R28   | 12.4          | 12.4         | 12.4         |
| R93   | 14            | 14           | 14           |
| R89   | 42.3          | 42.1         | 41.7         |
| R67   | 98.8          | 98.3         | 97.3         |
| R8    | 194           | 194          | 193          |
| R9    | 1950          | 1955         | 1933         |
| R10   | 1950          | 1955         | 1933         |

Table 17. L-L fault at bus 41

| Relay | PV 100% T(ms) | PV 75% T(ms) | PV 50% T(ms) |
|-------|---------------|--------------|--------------|
| R46   | 12.4          | 12.4         | 12.4         |
| R103  | 31            | 30.9         | 30.9         |
| R101  | 130           | 130          | 129          |
| R99   | 264           | 264          | 261          |
| R11   | 4265          | 4458         | 4502         |
| R12   | 4265          | 4458         | 4502         |
| R13   | 4265          | 4458         | 4502         |

#### 4.7. Distance relay (line to ground faults)

For the distance relay line-to-ground faults, different faults were made on several buses. This step is illustrated as shown in Tables 18-20. The distance relay was placed on the network cables instead of the overcurrent relay while changing the production rate of the photovoltaic cells. This step is performed in order to compare these results with the previous ones.

Table 18. L-G fault at bus 14

| Relay No | PV 100% T(ms) | PV 75% T(ms) | PV 50% T(ms) |
|----------|---------------|--------------|--------------|
| R25      | 14.3          | 14.3         | 14.4         |
| R89      | 80.5          | 84.6         | 88.6         |
| R67      | 170           | 184          | 199          |
| R8       | 295           | 330          | 367          |
| R9       | 3157          | 3617         | 4119         |
| R10      | 3157          | 3617         | 4119         |

Table 19. L-G fault at bus 19

| Relay No | PV 100% T(ms) | PV 75% T(ms) | PV 50% T(ms) |
|----------|---------------|--------------|--------------|
| R28      | 22.1          | 22.2         | 22.3         |
| R93      | 28.8          | 29.5         | 30.2         |
| R89      | 86.4          | 90.9         | 95.4         |
| R67      | 182           | 198          | 214          |
| R8       | 315           | 354          | 395          |
| R9       | 3419          | 3942         | 4517         |
| R10      | 3419          | 3942         | 4517         |

Table 20. L-G fault at bus 41

| Relay No | PV 100% T(ms) | PV 75% T(ms) | PV 50% T(ms) |
|----------|---------------|--------------|--------------|
| R46      | 15.9          | 15.9         | 16           |
| R103     | 69.6          | 71.4         | 73.3         |
| R101     | 267           | 283          | 298          |
| R99      | 479           | 524          | 571          |
| R11      | 4950          | 4950         | 4950         |
| R12      | 4950          | 4950         | 4950         |
| R13      | 4950          | 4950         | 4950         |

#### 4.8. Results and illustrations

In investigating the impact of changing the X/R ratio on the relay response speed, comparing results are presented in Tables 2-10. For instance, analyzing the response of relay 14 in Table 2 to a three-phase fault with varying reactance (values: 0.083, 0.12, and 0.185 Ohms) produce corresponding response times (ms): 144, 159, and 189, respectively, under 100% photovoltaic integration. This indicates that the relay response time increases with higher cable reactance, while noting that the optimum response time is observed at 144ms for a reactance value of 0.083 Ohms. Similarly, examining relay 8 in a three-phase fault at bus 14 with a 50% PV integration ratio and reactance values of: 0.083, 0.12, and 0.185 Ohms yields response times (ms) of: 658, 708, and 801, respectively, highlighting the fastest response time is when the cable reactance is minimized.

Considering the effect of varying the photovoltaic integration rates on the relay response time, results in Table 4 indicate a clear trend: an increase in integration rate leads to an increase in response time. For instance, the response speed (in ms) of relay 36 with a reactance of 0.083 Ohms is 151, 154, and 157 under 50%, 75%, and 100% PV output rates, respectively. This indicates that higher power production by the modules results in longer relay response times during three-phase and phase-to-phase failures. However, in the case of phase-to-ground faults, the response time increases with a decrease in the PV module production rate. The fault type does not alter this trend, as consistent results across various fault types indicate that relay response speed improves with lower cable reactance values.

Simulation results additionally reveal that employing distance relays instead of overcurrent relays on cables enhances response time. A comparison between the distance relay 89 and the overcurrent relay 21 in Tables 11-12 for a three-phase fault at 100% energy production with a reactance of 0.083 Ohms demonstrates a response time of 40.6 milliseconds for the distance relay, outperforming the overcurrent relay's 58.7 milliseconds. This improvement, achieved by adjusting cable reactance values, underscores the superiority of distance relays regarding response time, as consistently indicated in Tables 12-20. With all such observations, it is important now to say that the motivation behind selecting the proposed method, which is using the distance relay instead of the overcurrent relay and changing the reactance, maybe illustrated by the following points:

- Detection principle and measurement: Distance relays use voltage and current signals to calculate an apparent fault impedance, which helps in locating the fault geographically. This makes the distance relay inherently faster and more accurate (for detecting faults in distribution lines) than the overcurrent relays which only measure high currents.
- Load flows and renewable integration: Distance relays are directional and thus can differentiate between forward and reverse flows. This makes them better suited for distribution grids with high renewable penetration while fault current directions may vary.
- Adaptability: Distance relays are numerically calibrated where settings can be easily adapted as the distribution network configuration changes over time with the additions of distributed generation sources.
- Reliability: Distance relays are less prone to problems such as protection blinding and sympathy tripping, which overcurrent relays often suffer from due to intermittent faults and power swings.
- Coordination complexity: Although the initial installation requires comprehensive modeling and simulation, distance relays ease the overall protection coordination burden for the ever-evolving distribution grid compared with other alternatives.

Furthermore, based on an economic feasibility approach aimed at achieving better response time at the lowest cost, comparison results are presented in Table 21. The comparison, as an example shown in this table, demonstrates that replacing cables with lower reactance is substantially more expensive than changing the overcurrent relay and adopting distance relays. The total cost of cables is calculated by multiplying the price per meter (\$31.24) by 147,000m, resulting in \$4,592,280, with an additional 20% for installation costs, yielding \$5,510,736. Now, the total cost of installing 22 distance relays is approximately \$484,000. Therefore, replacing the overcurrent relay with distance relays not only achieves a faster response time but also cost saving. That is, \$5,510,736-\$484,000 = \$5,026,736 of saved money while using distance relays instead of replacing all cables. The alternative of replacing all cables is deemed impractical due to the



associated challenges, such as time, effort, and cost, especially in inaccessible locations like tunnels and remote areas. On the other hand, for the overcurrent relay replacement, it is noted that with each relay priced at approximately \$3,000, a total cost of \$66,000, offering a more budget-friendly option that can be allocated to other areas of the network.

Table 21. Elements cost comparisons

| Item              | Cross-section (mm <sup>2</sup> ) | Number of cores | Unit cost (USD/km) | Quantity       | Total price (USD) |
|-------------------|----------------------------------|-----------------|--------------------|----------------|-------------------|
| Cables            | 240                              | 1               | 31.24              | 147,000 meters | 5,510,736         |
| Distance relay    | ---                              | ---             | 20,000             | 22             | 484,000           |
| Overcurrent relay | ---                              | ---             | 3000               | 22             | 66000             |

## 5. CONCLUSION

In this paper, an investigation of protection system improvement in distribution networks integrated with photovoltaic cells is presented. The protection system improvement is achieved by changing the impedance to resistance ratio values of the network cables. Simulation results show that the response speed of the overcurrent relay can be enhanced by utilizing cables with relatively low X/R ratios, notably a decrease in cable reactance correlates with an increase in relay response speed. This relationship remains consistent regardless of the type of failure, as results show that the fastest response time is consistently associated with the lowest cable reactance value. Furthermore, the investigation reveals that an increase in energy production from renewable energy units can be extended to the response time of the relay in the case of three-phase or phase-to-phase failures. However, in cases of phase-to-ground failures, results indicate a contrary trend where higher energy production leads to a reduction in relay response time. Moreover, simulation results affirm the feasibility of employing a distance relay as a viable alternative to the overcurrent relay, providing improved fault response times. These discoveries offer valuable insights into optimizing relay performance within the framework of renewable energy integration.

## ACKNOWLEDGEMENTS

The authors would like to sincerely thank the anonymous reviewers for their valuable comments, which indeed raised the level of the article presentation. The corresponding author would also like to thank The University of Jordan for granting a sabbatical leave and the Al-Ahliyya Amman University for supporting this research.




## REFERENCES

- [1] A. H. Numan, Z. S. Dawood, and H. A. Hussein, "Theoretical and experimental analysis of photovoltaic module characteristics under different partial shading conditions," *International Journal of Power Electronics and Drive Systems (IJPEDS)*, vol. 11, no. 3, pp. 1508–1518, Sep. 2020, doi: 10.11591/ijpeds.v11.i3.pp1508-1518.
- [2] A. M. Baniyounes, G. Liu, M. G. Rasul, and M. K. Khan, "Solar desiccant cooling and indoor air quality for institutional building in subtropical climate (review)," 2012. doi: 10.2316/P.2012.768-091.
- [3] A. Mularczyk, I. Zdonek, M. Turek, and S. Tokarski, "Intentions to use prosumer photovoltaic technology in Poland," *Energies*, vol. 15, no. 17, p. 6300, Aug. 2022, doi: 10.3390/en15176300.
- [4] A. Elkhatat and S. A. Al-Muhtaseb, "Combined 'renewable energy–thermal energy storage (RE–TES)' systems: a review," *Energies*, vol. 16, no. 11, p. 4471, Jun. 2023, doi: 10.3390/en16114471.
- [5] A. Marciniuk-Kluska and M. Kluska, "Forecasting energy recovery from municipal waste in a closed-loop economy," *Energies*, vol. 16, no. 6, p. 2732, Mar. 2023, doi: 10.3390/en16062732.
- [6] P. Ifaei, A. S. Tayerani Charmchi, J. Loy-Benitez, R. J. Yang, and C. Yoo, "A data-driven analytical roadmap to a sustainable 2030 in South Korea based on optimal renewable microgrids," *Renewable and Sustainable Energy Reviews*, vol. 167, p. 112752, Oct. 2022, doi: 10.1016/j.rser.2022.112752.
- [7] Z. Li, J. Guo, X. Gao, X. Yang, and Y.-L. He, "A multi-strategy improved sparrow search algorithm of large-scale refrigeration system: Optimal loading distribution of chillers," *Applied Energy*, vol. 349, p. 121623, Nov. 2023, doi: 10.1016/j.apenergy.2023.121623.
- [8] S. Acharya, "Analytic assessment of renewable potential in Northeast India and impact of their exploitation on environment and economy," *Environmental Science and Pollution Research*, vol. 29, no. 20, pp. 29704–29718, Apr. 2022, doi: 10.1007/s11356-022-18498-3.
- [9] S. Abdallah, M. Abu-Hilal, and M. S. Mohsen, "Performance of a photovoltaic powered reverse osmosis system under local climatic conditions," *Desalination*, vol. 183, no. 1–3, pp. 95–104, Nov. 2005, doi: 10.1016/j.desal.2005.03.030.
- [10] A. Ghaffari, A. Askarzadeh, and R. Fadaeinedjad, "Optimal allocation of energy storage systems, wind turbines and photovoltaic systems in distribution network considering flicker mitigation," *Applied Energy*, vol. 319, p. 119253, Aug. 2022, doi: 10.1016/j.apenergy.2022.119253.
- [11] S. K. Das, S. Sarkar, and D. Das, "Performance enhancement of grid-connected distribution networks with maximum penetration of optimally allocated distributed generation under annual load variation," *Arabian Journal for Science and Engineering*, vol. 47, no. 11, pp. 14809–14839, Nov. 2022, doi: 10.1007/s13369-022-06951-x.
- [12] S. A. Aleem, S. M. S. Hussain, and T. S. Ustun, "A review of strategies to increase PV penetration level in smart grids," *Energies*, vol. 13, no. 3, p. 636, Feb. 2020, doi: 10.3390/en13030636.
- [13] Y. Yue, "Making urban power distribution systems climate-resilient," Manila, Philippines, May 2022. doi: 10.22617/WPS220221.




- [14] H. Agarwal, "Protection coordination of distribution system with distributed generation," 2022.
- [15] Y. N. Velaga, R. Jain, and J. Sawant, "Modeling distributed energy resources for analyzing distribution systems with high renewable penetration," in *2022 IEEE Rural Electric Power Conference (REPC)*, Apr. 2022, pp. 11–17. doi: 10.1109/REPEC55671.2022.00011.
- [16] S. Chowdhury, S. P. Chowdhury, and P. Crossley, *Microgrids and active distribution networks*. The Institution of Engineering and Technology, 2009.
- [17] A. Salah Saidi, "Impact of grid-tied photovoltaic systems on voltage stability of tunisian distribution networks using dynamic reactive power control," *Ain Shams Engineering Journal*, vol. 13, no. 2, p. 101537, Mar. 2022, doi: 10.1016/j.asej.2021.06.023.
- [18] D. Kim *et al.*, "Importance of channel dimension for flow-electrode flowing in flow-electrode capacitive mixing (F-CapMix): Evaluation of net power density under high-pressure-drop conditions," *Separation and Purification Technology*, vol. 290, p. 120859, Jun. 2022, doi: 10.1016/j.seppur.2022.120859.
- [19] M. Barboura and A. Bouras, "Resilience, criticality and operating limits of a MALT 30 kV 4-wire electrical distribution network without conformity of the medium voltage neutral," *IET Generation, Transmission & Distribution*, vol. 16, no. 16, pp. 3349–3362, Aug. 2022, doi: 10.1049/gtd2.12507.
- [20] A. Sil and S. Maity, *Industrial power system evolutionary aspects*. 2022. doi: 10.1201/9781003231240.
- [21] X. Li, H. Dong, J. Liu, X. Lin, and Z. Sun, "Synergetic control strategy of front-end speed regulation wind turbine (FESRWT) for fault ride through," *Mathematical Problems in Engineering*, vol. 2022, pp. 1–11, Mar. 2022, doi: 10.1155/2022/6150753.
- [22] X.-Y. Zhong, G.-W. Yan, and Z.-H. Chen, "Structure and energy storage properties of (1-x)Ba<sub>0.98</sub>Li<sub>0.02</sub>TiO<sub>3</sub> based ceramics with xBi(Mg<sub>1/2</sub>Sn<sub>1/2</sub>)O<sub>3</sub> addition," *Journal of Alloys and Compounds*, vol. 891, p. 161855, Jan. 2022, doi: 10.1016/j.jallcom.2021.161855.
- [23] H. Shakibi, S. Afzal, A. Shokri, and B. Sobhani, "Utilization of a phase change material with metal foam for the performance improvement of the photovoltaic cells," *Journal of Energy Storage*, vol. 51, p. 104466, Jul. 2022, doi: 10.1016/j.est.2022.104466.
- [24] S. Kotb, A. Eisa, M. Zaky, and A. Adly, "An evaluation of the ETRR2's electrical power system short circuit study using ETAP software," *Arab Journal of Nuclear Sciences and Applications*, vol. 55, no. 2, pp. 125–134, Apr. 2022, doi: 10.21608/ajnsa.2022.93854.1509.
- [25] A. F. O. and I. N. S., "Short circuit analysis of a Nigerian 132/33 kV injection substation," *Advances in Engineering Design Technology*, vol. 4, no. 1, pp. 1–10, 2022, doi: <https://doi.org/10.37933/nipes.a/4.1.2022.1>.
- [26] H. Al-bayaty, M. S. Kider, O. N. Jasim, and A. Shakor, "Electrical distribution grid of Kirkuk City: A case study of load flow and short circuit valuation using ETAP," *Periodicals of Engineering and Natural Sciences*, vol. 10, no. 3, pp. 311–322, 2022, [Online]. Available: <http://pen.ius.edu.ba/index.php/pen/article/viewFile/3029/1176>.

## BIOGRAPHIES OF AUTHORS






**Muhanad N. Ali**    earned his bachelor's degree in electrical power engineering from Diyala University in 2002, before completing his master's degree in electrical engineering from the University of Jordan, Jordan, in 2022. He is currently a manager of the solar power plant project in Anbar/Iraq. His research interests lie in renewable energy, solar power systems, community-based projects, environmental sustainability, and photovoltaic technologies. He can be contacted at email: [eng.muhanad79@gmail.com](mailto:eng.muhanad79@gmail.com).



**Othman M. K. Alsmadi**    graduated from Tennessee State University in 1993 with a B.S. in electrical engineering and an M.S. degree in 1995. In 1999, he received his Ph.D. from Wichita State University. Currently, he is the department chair at the Al-Ahliyya Amman University with a sabbatical leave from The University of Jordan. Prof. Alsmadi's research interests include optimal control, model order reduction, system identification, neural networks, and artificial intelligence techniques. He can be contacted at email: [othmanmk@ju.edu.jo](mailto:othmanmk@ju.edu.jo).



**Ali M. Baniyounes**    is an associate professor and the former chair of the Electrical Engineering Department at Applied Science Private University, Amman-Jordan. He obtained his B.S. in electrical engineering from Yarmouk University, at Jordan in 1997, the M.S. in computer control engineering from the University of Technology Sydney, Australia in 2004. He joined CQ university, Australia in 2009. His areas of interest are power engineering, adaptive, fuzzy and intelligent control, and engineering education. He can be contacted at email: [al\\_younes@asu.edu.jo](mailto:al_younes@asu.edu.jo).